THE INFLUENCE OF EQUATORIAL WAVES ON QUIKSCAT WINDS IN THE ATLANTIC

Paulo S. Polito[1], Olga T. Sato[1] and W. Timothy Liu[2]

[1] Earth Observation Department
INPE - National Institute for Space Research, Brazil

[2] Jet Propulsion Laboratory
California Institute of Technology

INTRODUCTION

Scatterometer measurements depend on the sea surface roughness which is in principle caused by the **wind stress against a static ocean surface**.

Alternatively, a **moving ocean against the static atmosphere** can have the same effect.

[4] has shown that currents linked to Tropical Instability Waves (TIWs) induce a signal in the scatterometer winds in the eastern tropical Pacific.

This study investigates the hypothesis that surface currents associated with TIWs and equatorial Rossby waves can **bias the QuikScat scatterometer winds** in the region of the **PIRATA** buoys in the Atlantic.

THEORY

TIWs are Rossby-gravity waves generated by barotropic instability. These waves are seasonally and interannually modulated by equatorial currents.

TIWs zonal phase speed (c_p), wavelength (λ) and period (P) are on the order of **-35 km day^{-1}, 1000 km and one month** [6]. These attributes can vary by more than a factor of 2.

1^{st} order theory indicates zonal propagation thus meridional geostrophic **currents** v_g arise associated with the **slopes** of the surface.

$$v_g = \frac{g}{f}\frac{\partial \eta}{\partial x}, \qquad (1)$$

Geostrophy does not apply at (or at few degrees of) the equator because f is evanescent.

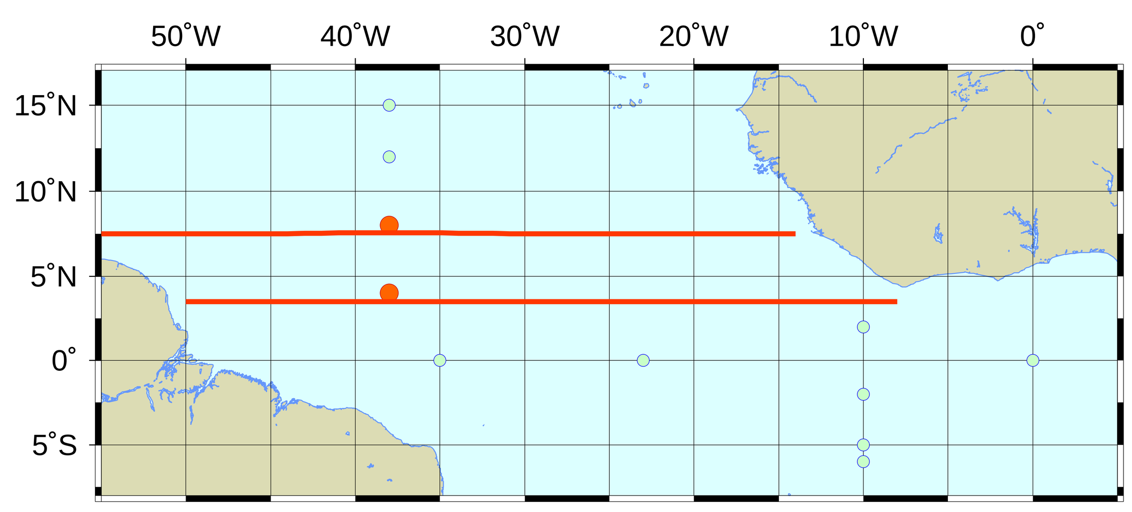

Figure 1: **Pilot Research Moored Array in Tropical Atlantic (PIRATA)** buoys (circles) and **TOPEX/POSEIDON (T/P)** latitudinal bands (lines). Locations studied in detail are red, others are blue.

METHODS

WINDS The **in–situ** winds v_{pi} between 3/00 and 5/01 are daily averages of PIRATA buoy measurements, available on–line.

The 12h $\times$ 1/4° interpolated **QuikScat** winds v_{qs} are distributed by JPL/PODAAC.

The **difference** $\Delta_v = v_{pi} - v_{qs}$ between meridional wind components from **PIRATA and QuikScat** measurements is calculated from winds that are measured in the **same day** and are up to **28 km** apart.

v_{pi} and v_{qs} are referred to heights of **4 and 10 m.** v_{pi} is multiplied by a constant such that the corrected v_{pi} explains the most variance from v_{qs}.

HEIGHT The waves are detected by the T/P altimeter in the PIRATA region. The corrected sea surface height anomaly η is calculated in relation to an 8–year average (1993–2000), is bicubically interpolated to a 1°$\times$ 1° grid and stored as $\eta_o(x,t)$.

Finite impulse response filters decompose $\eta_o(x,t)$ into spectral bands associated with:

- η_t $\rightarrow$ Basin–wide, non–propagating signal (mostly seasonal)
- $\eta_{24,12,6,3}$ $\rightarrow$ Long 1^{st} mode **Rossby waves** ($P =$ 24, 12, 6 and 3 months)
- η_1 $\rightarrow$ **Tropical instability waves** ($P =$ 1.5 months)
- $\eta_{K6,K3,K1}$ $\rightarrow$ Equatorial Kelvin waves ($P =$ 6, 3 and 1.5 months)
- $\eta_{E,r}$ $\rightarrow$ meso–scale eddies and a small scale residual

$$\text{i.e.: } \eta_o = \eta_t + \eta_{24} + \eta_{12} + \eta_6 + \eta_3 + \eta_1 + \eta_{K6} + \eta_{K3} + \eta_{K1} + \eta_E + \eta_r. \qquad (2)$$

This method is described in detail in [5].

The **meridional current** v_g is estimated based on the filtered T/P components η_3 and η_1, (smaller L $\Rightarrow$ stronger currents).

COMPARISON Δv **is smoothed** with a spline–based routine whose tension is adjusted to maximize their cross–correlation c with v_g.

c is calculated for all buoys and its statistical significance is obtained by Monte Carlo simulations based on the the number of **original** T/P samples.

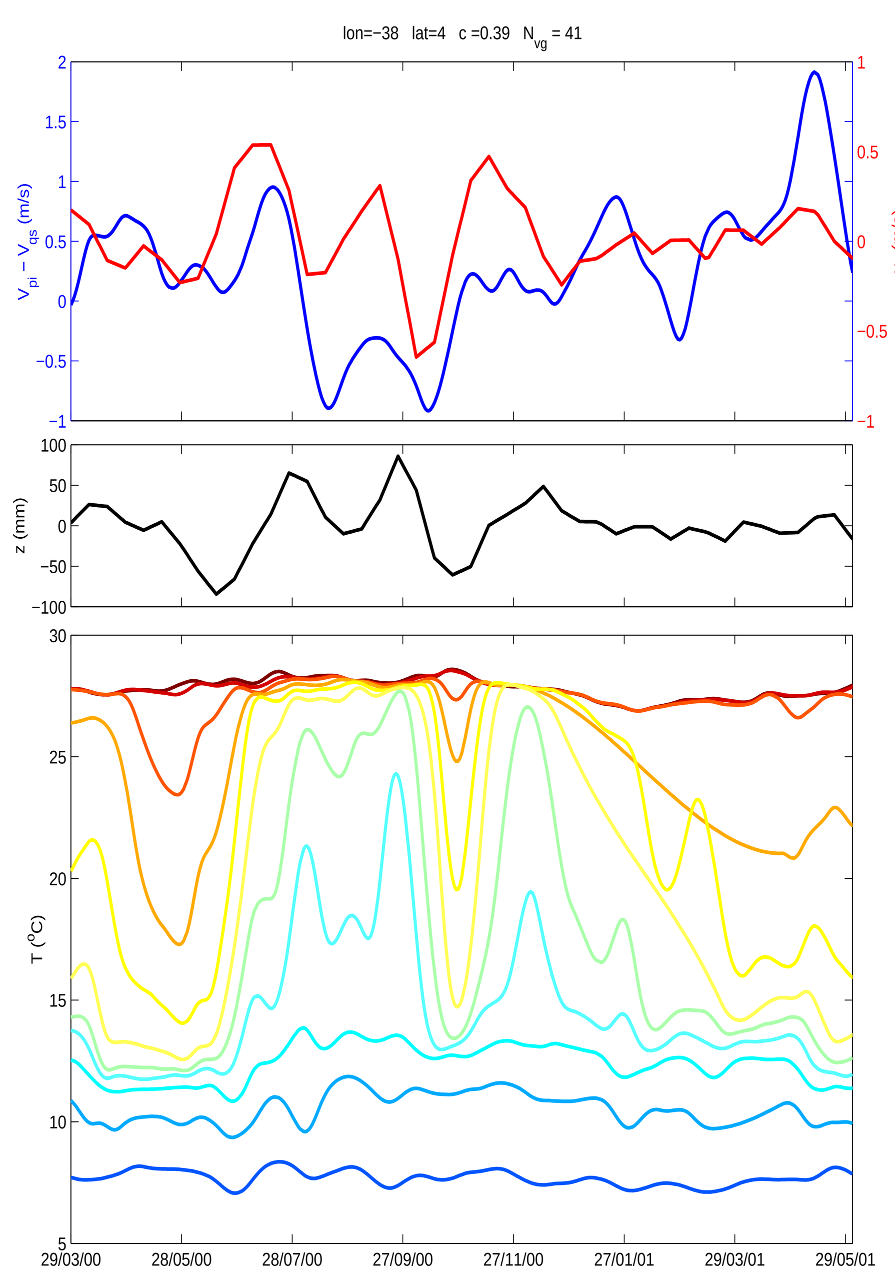

Figure 2: Results from QuikScat, TOPEX/POSEIDON and the PIRATA buoy at 38° W, 4° N.

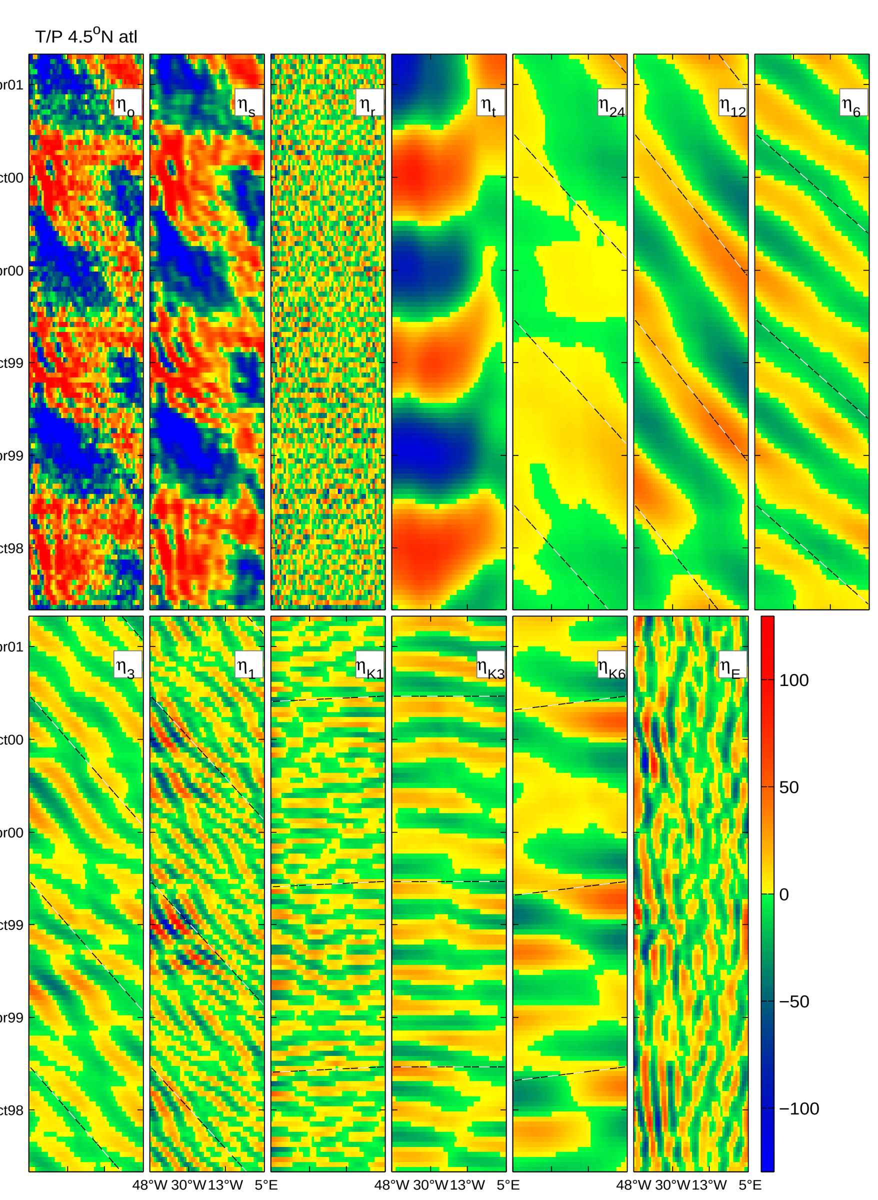

Figure 3: Original (η_o), sum of filtered (η_s), residual (η_r), and filtered sea surface height anomaly fields (η_t, η_{24}, η_{12}, η_6,η_3,η_1, η_{K1}, η_{K3},η_{K6} and η_E), as in Equation 2 at 3.5° N in the Atlantic, in mm. Dash-dot lines are estimates for mean zonal phase speed.

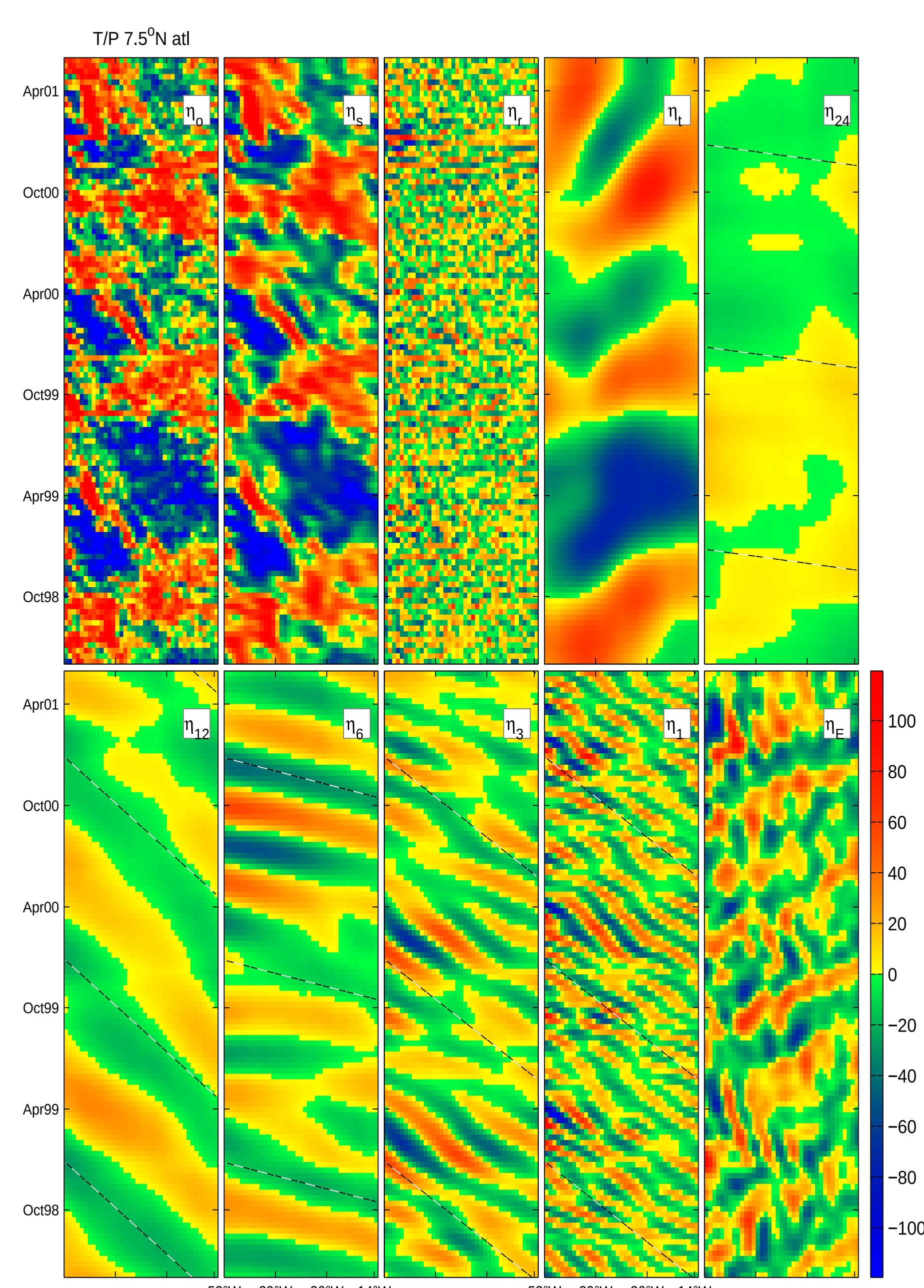

Figure 4: Same as Figure 3 but for 7.5° N.

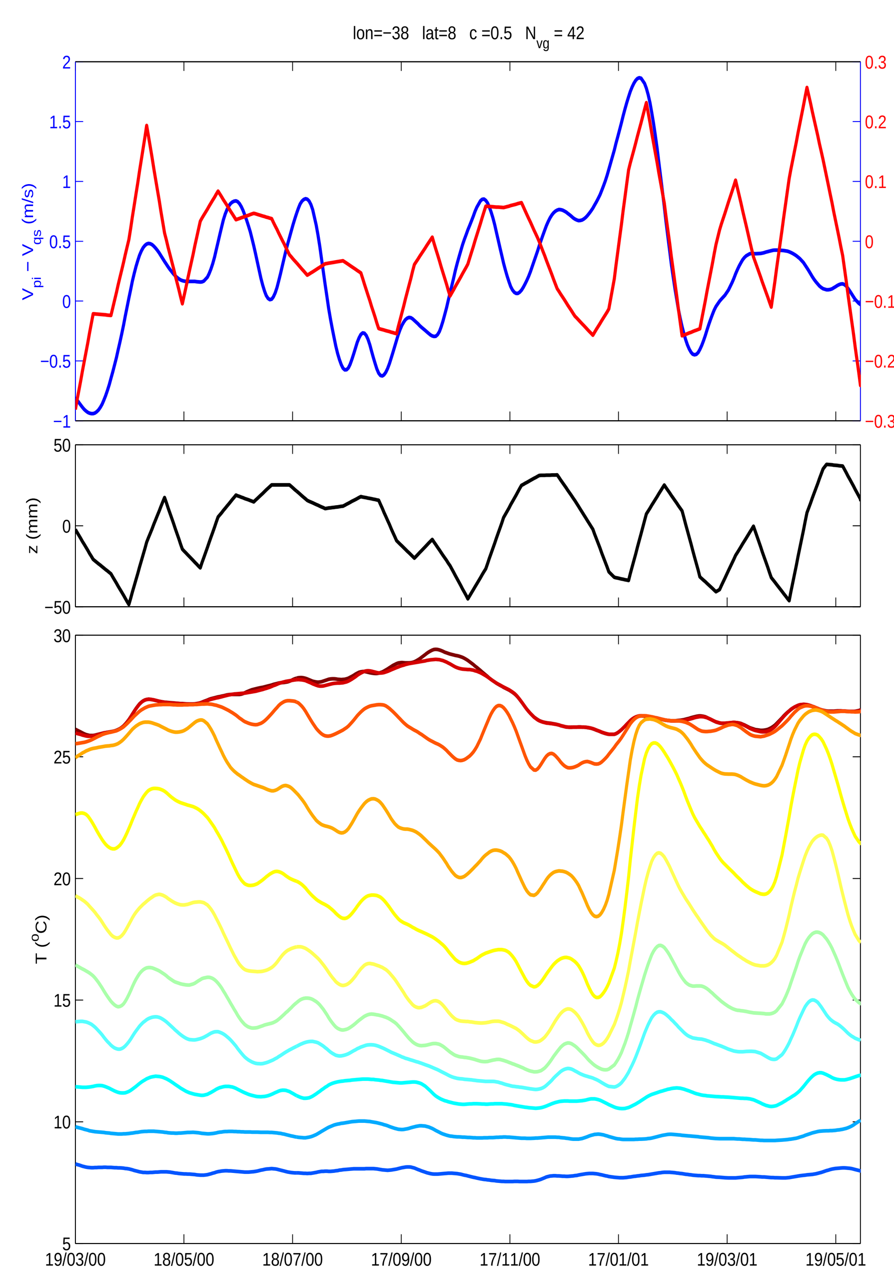

Figure 5: Results from QuikScat, TOPEX/POSEIDON and the PIRATA buoy at 38° W, 8° N.

RESULTS

Longitude	Latitude	c	N_{vg}
0°	0°	.17	25
10° W	0°	-.06	28
10° W	2° S	-.31	9
10° W	5° S	-.75	11
10° W	6° S	.03	42
10° W	10° S	-.04	29
10° W	2° N	.42	9
23° W	0°	.34	44
35° W	0°	.18	37
38° W	**4° N**	**.39**	**41**
38° W	**8° N**	**.50**	**42**
38° W	12° N	-.07	46
38° W	15° N	-.31	20

Table 1 shows the correlation c and the number of original T/P samples N_{vg}. The 2 buoys in bold are the red circles in Figure 1, selected because they **(1)** have long time series, **(2)** are far from the equator and **(3)** c is statistically significant at a 95% confidence level.

In **Figure 2** the top plot shows the positive correlation between Δ_v and v_g. The middle plot shows sea surface height anomaly associated with trimestral Rossby waves (η_3) and TIWs (η_1). The bottom plot shows temperature time series for thermistors at 1, 20, 40, 60, 80, 100, 120, 140, 180, 300 and 500 m, from red to blue.

The **magnitude** of v_g is similar to that of Δ_v.

Figure 3 shows a dominant seasonal signal η_t and very clear annual and semiannual Rossby waves (η_{12}, η_6). Kelvin wave components (η_{K1}, η_{K3}, and η_{K6}) are not well defined. **TIWs** (η_1) show energetic bursts on October of 1999 and 2000. The **trimestral Rossby waves** (η_3) bursts occur approximately two months earlier.

η_3 and η_1 have average phase speeds (-23 and -24 km/day), periods (124 and 57 days) and wavelengths (2852 and 1368 km) within the expected range. The TIW signal that T/P can capture is on the low–frequency end of the TIW spectrum, due to its **10 day sampling rate.**

A stronger argument comes from the buoy at 38° W, 8° N, **Figure 5.** c is larger than at 38° W, 4° N although Δv (top, blue line) shows more variability than the T/P–derived v_g (red line). This is probably due to the **sampling rate difference.** The PIRATA data, particularly the yellow and green curves between 60 and 100 m in 1999 and 2000, show wave–like variability with $\sim$ one month period, a signal not fully captured by the T/P altimeter.

In **Figure 4** the η_1 signal shows pulses of high amplitude centered approximately on March of 1999, 2000 and, with less intensity, 2001. The η_3 signals occur approximately one month earlier.

The bottom plots of Figures 2 and 5 show the vertical structure of Rossby waves and TIWs.The surface layer (1 m, dark red) temperature variability is **dominated by the seasonal signal,** while the variability at the frequency bands of η_3 and η_1 has an amplitude of a **fraction of a degree.** The amplitude of the wave–like temperature signal at 80 m is **up to 7° C** in 2001.

CONCLUSIONS

Significant correlations between Δ_v and v_g are observed at 4° N, 38° W and 8° N, 38° W.

At these two latitudes **TIWs are very clear** in the filtered T/P record. The PIRATA temperature profiles corroborate these observations.

The presented evidences suggest that a significant part of the wind difference is **not random** . Instead, it is a **bias** introduced by ocean currents associated with TIWs and Rosby waves.

The alternative hypothesis to explain the influence of TIWs in the wind is based on the **enhanced vertical mixing and depends on sea surface temperature anomalies** ([7],[2], and later [1], [3]).

Figures 2 and 4 show that the **SST variability is weak** and issurpassed by that of the sub–surface layer by one order of magnitude. These evidences suggest that this hypothesis does not hold in the 2 selected buoy locations.

Although scatterometer winds are probably biased by the surface currents, the scatterometer **stress** is correct and includes the contribution from the moving ocean surface.

e-mail for contact: polito@ltid.inpe.br

References

[1] D. B. Chelton, F. J. Wentz, C. L. Gentemann, R. A. de Szoeke, and M. G. Schlax. Satellite microwave sst observation of transequatorial tropical instability waves. *Geophysical Research Letters*, 27:1239–1242, 2000.

[2] S. P. Hayes, M. J. McPhaden, and J. M. Wallace. The influence of sea surface temperature on surface wind in the eastern equatorial Pacific. *Journal of Climate*, 2:1500–506, 1989.

[3] W. T. Liu, X. Xie, P. S. Polito, S.-P. Xie, and H. Hashizume. Atmospheric manifestation of tropical instability wave observed by QuikSCAT and Tropical Rain Measuring Mission. *Geophysical Research Letters*, 27:2545–2548, 2000.

[4] P. S. Polito, J. P. Ryan, W. T. Liu, and F. P. Chavez. Oceanic and atmospheric anomalies of tropical instability waves. *Geophysical Research Letters*, 28(11):2233–2236, 2001.

[5] P. S. Polito, O. T. Sato, and W. T. Liu. Characterization and validation of heat storage variability from Topex/Poseidon at four oceanographic sites. *Journal of Geophysical Research*, 105(C7):16,911–16,921, 2000.

[6] L. Qiao and R. H. Weisberg. Tropical instability wave kinematics: observations from the tropical instability wave experiment (TIWE). *Journal of Physical Oceanography*, 100:8677–8693, 1995.

[7] J. M. Wallace, T. P. Mitchell, and C. Deser. The influence of sea surface temperature on surface wind in the eastern equatorial Pacific: Seasonal and interannula variability. *Journal of Climate*, 2:1492–1499, 1981.